nature cell biology

Heart field origin of great vessel precursors relies on *nkx2.5*-mediated vasculogenesis

Noëlle Paffett-Lugassy[1,2,3], Reena Singh[4], Kathleen R. Nevis[1,2], Burcu Guner-Ataman[1,2], Evan O'Loughlin[1,2], Leila Jahangiri[1,2], Richard P. Harvey[4], C. Geoffrey Burns[1,2,3,5] and Caroline E. Burns[1,2,3,5]

The pharyngeal arch arteries (PAAs) are transient embryonic blood vessels that make indispensable contributions to the carotid arteries and great vessels of the heart, including the aorta and pulmonary arteries[1,2]. During embryogenesis, the PAAs appear in a craniocaudal sequence to connect pre-existing segments of the primitive circulation after *de novo* vasculogenic assembly from angioblast precursors[3,4]. Despite the unique spatiotemporal characteristics of PAA development, the embryonic origins of PAA angioblasts and the genetic factors regulating their emergence remain unknown. Here, we identify the embryonic source of PAA endothelium as *nkx2.5*$^{+}$ progenitors in lateral plate mesoderm long considered to adopt cell fates within the heart exclusively[5,6]. Further, we report that PAA endothelial differentiation relies on Nkx2.5, a canonical cardiac transcription factor not previously implicated in blood vessel formation. Together, these studies reveal the heart field origin of PAA endothelium and attribute a new vasculogenic function to the cardiac transcription factor Nkx2.5 during great vessel precursor development.

During the course of analysing zebrafish embryos expressing a yellow fluorescent protein from *nkx2.5 cis*-regulatory sequences (*Tg(nkx2.5:ZsYellow)*) (ref. 7), we observed fluorescence in known *nkx2.5*$^{+}$ organs including the heart and liver (Fig. 1a and Supplementary Fig. 2a). Unexpectedly, we also observed ZsYellow fluorescence in pharyngeal structures revealed through co-localization studies to be endothelial cells comprising PAAs 3–6 and the adjoining ventral aorta (Fig. 1a–d). Among the embryonic vasculature, only the PAAs and ventral aorta expressed ZsYellow consistent with their unique developmental origin[3,4]. To pursue this observation further, we followed the dynamics of ZsYellow fluorescence during developmental stages leading up to PAA establishment. During mid-somitogenesis, we observed ZsYellow in bilateral populations of anterior lateral plate mesoderm (ALPM) previously identified as ventricular myocardial precursors in the zebrafish heart-forming region[6,8] (Fig. 1e and Supplementary Fig. 2b,c,g–j). As expected, ventricular precursors migrated medially and contributed to the heart. Interestingly, fractions of the ZsYellow^{+} field remained lateral and condensed by 28 h post-fertilization (hpf) into pharyngeal clusters (Fig. 1f,g) that we verified were non-endodermal (Fig. 1h and Supplementary Fig. 2d–f).

To rule out a position effect of the transgene, we confirmed that *nkx2.5* transcripts also localized to pharyngeal clusters at 28 hpf (Fig. 1i and Supplementary Fig. 2k,l). Over the next 20 h, however, *nkx2.5* transcripts progressively disappeared in a craniocaudal sequence until expression was undetectable specifically in the pharynx at 48 hpf (Fig. 1j–l and Supplementary Fig. 2m,o). In contrast, ZsYellow transcripts persisted longer in *Tg(nkx2.5:ZsYellow)* embryos, thereby providing an explanation for the robust ZsYellow fluorescence observed in PAAs 3–6 (Supplementary Fig. 2m–p). Intriguingly, a previous report[3] described the cranial to caudal appearance of four *tie1*$^{+}$ PAA angioblast clusters in pharyngeal mesoderm during a developmental window overlapping with the cranial to caudal disappearance of *nkx2.5*$^{+}$ clusters that we observed (Fig. 1j–l). Using double *in situ* hybridization, we revealed a reciprocal relationship between *nkx2.5* and *tie1* transcripts in each pharyngeal cluster (Fig. 1m–p). Specifically, *nkx2.5* expression precedes that of *tie1* (Fig. 1m), yet after a transient period of overlap, *nkx2.5* transcripts decline whereas *tie1* expression is maintained throughout PAA morphogenesis[3] (Fig. 1n–p). These data suggest that *tie1*$^{+}$ PAA angioblasts derive from undifferentiated *nkx2.5*$^{+}$ clusters in the pharynx.

To begin testing this hypothesis, we tracked the derivatives of *nkx2.5*$^{+}$ clusters expressing the photoconvertible kaede protein, which instantly switches from green to red fluorescence following ultraviolet light exposure[9]. Pan-kaede photoconversion at 30 hpf resulted in robust red fluorescence in PAAs 3 and 4 with regions of red and green fluorescence or green-only fluorescence in PAAs 5 and 6 (Fig. 2a–d). On the basis of the red and green fluorescent signal distributions,

[1]Cardiovascular Research Center, Massachusetts General Hospital, Charlestown, Massachusetts 02129, USA. [2]Harvard Medical School, Boston, Massachusetts 02115, USA. [3]Harvard Stem Cell Institute, Cambridge, Massachusetts 02138, USA. [4]Victor Chang Research Institute, Darlinghurst, New South Wales 2010, Australia. [5]Correspondence should be addressed to C.G.B. or C.E.B. (e-mail: gburns@cvrc.mgh.harvard.edu or cburns6@partners.org)

Received 4 February 2013; accepted 18 September 2013; published online 27 October 2013; DOI: 10.1038/ncb2862

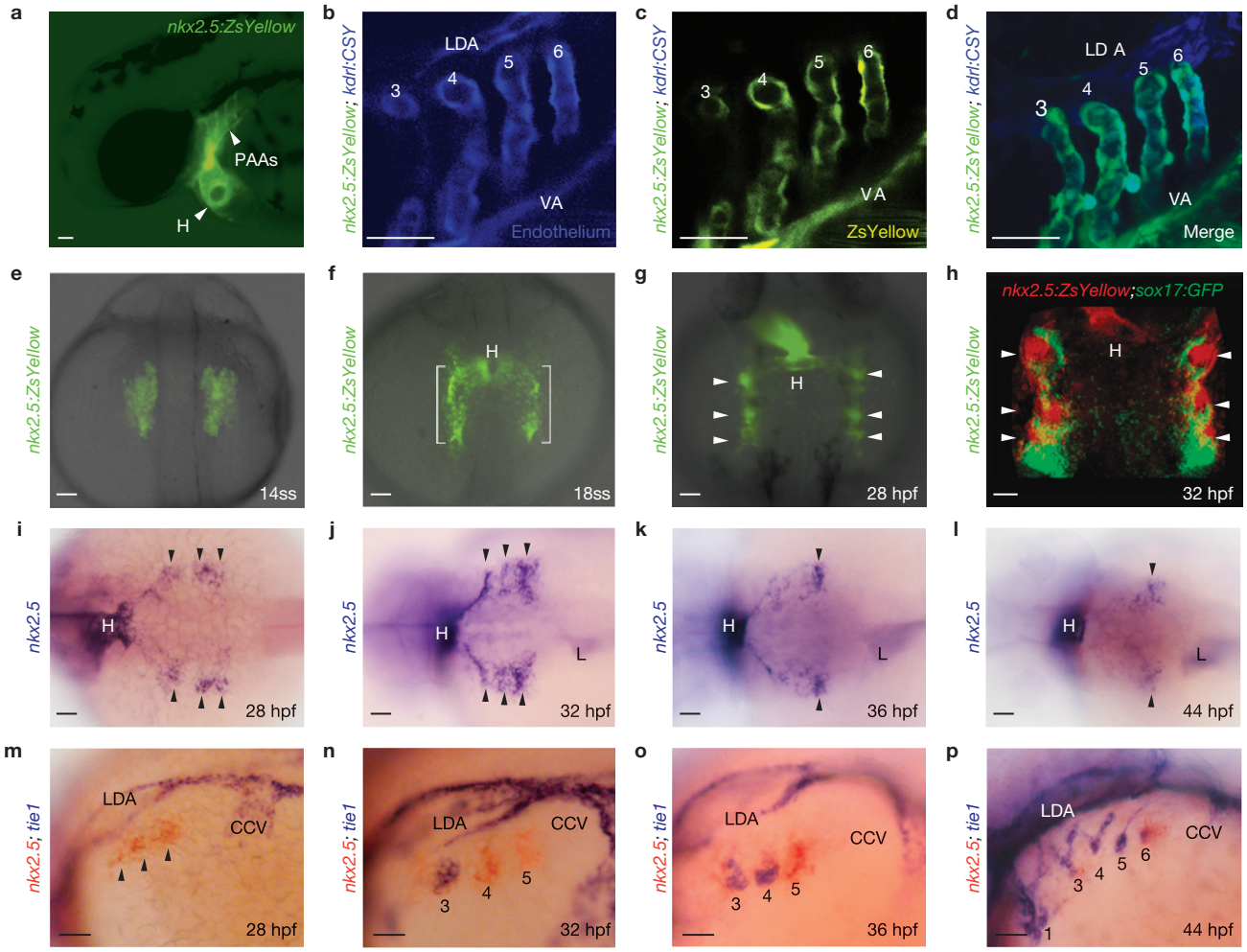

Figure 1 *nkx2.5* is expressed in presumptive PAA endothelial progenitors. (**a**) A *Tg(nkx2.5:ZsYellow)* embryo at 60 hpf exhibiting fluorescence in the heart and PAAs. (**b**–**d**) A *Tg(nkx2.5:ZsYellow); Tg(kdrl:CSY)* embryo at 60 hpf with overlapping yellow and blue fluorescence in the endothelium of PAAs 3–6 and the ventral aorta. The LDA exhibits blue fluorescence exclusively. (**e**–**g**) ZsYellow fluorescence in *Tg(nkx2.5:ZsYellow)* embryos at the 14-somite stage (**e**), 18-somite stage (**f**) and 28 hpf (**g**). Brackets and arrowheads highlight non-cardiogenic *nkx2.5*$^{+}$ cells in the pharynx. (**h**) A *Tg(nkx2.5:ZsYellow); Tg(sox17:GFP)* embryo at 32 hpf with *nkx2.5*$^{+}$ pharyngeal cells (red) and *sox17*$^{+}$ pharyngeal endoderm (green). (**i**–**l**) *In situ* hybridization time course of *nkx2.5* expression in the pharynx. Arrowheads mark *nkx2.5*$^{+}$ pharyngeal clusters. (**m**–**p**) Double *in situ* hybridization time course of *nkx2.5* (red) and *tie1* (blue) expression. PAA1 (labelled in **p**) forms earlier in development and never expresses *nkx2.5*. *tie1*$^{+}$ clusters are numbered according to the mature PAA they derive. Scale bars, 50 μm. Lateral views, anterior left (**a**–**d**,**m**–**p**); dorsal views, anterior up (**e**–**h**); dorsal views, anterior left (**i**–**l**); $n > 20$ embryos per group (**a**–**p**). VA, ventral aorta; LDA, lateral dorsal aorta; ss, somite stage; hpf, hours post-fertilization; H, heart; L, liver; CCV, common cardinal vein.

we conclude that PAAs 3 and 4 derive exclusively from progenitor cells that express *nkx2.5* before photoconversion at 30 hpf. In contrast, only a small fraction of PAAs 5 and 6 derive from cells expressing *nkx2.5* before photoconversion with most progenitors initiating *nkx2.5* expression thereafter.

To determine whether each *nkx2.5*$^{+}$ cluster gives rise to a single PAA, we individually traced their cell fates using focused kaede photoconversion. At 30 hpf, three bilateral pairs of *nkx2.5*$^{+}$ clusters were visualized in pharyngeal mesoderm (Fig. 2e). The second cluster gives rise exclusively to PAA3 (Fig. 2e,f). The third cluster, and scattered cells located caudal to the third cluster, become PAA4 and part of PAA5 (Supplementary Fig. 3a–c). Between 30 and 44 hpf, we witnessed the caudal emergence of two new kaede^{+} clusters that when photoconverted individually, resulted in PAAs 5 or 6 being labelled exclusively with red fluorescence (Fig. 2g,h). These findings support our hypothesis that individual *nkx2.5*$^{+}$ clusters give rise to single PAAs and that most progenitors for the caudal-most PAAs are specified after 30 hpf.

On the basis of the apparent segregation of ZsYellow^{+} pharyngeal clusters from myocardial precursors in the ALPM of *Tg(nkx2.5:ZsYellow)* embryos (Fig. 1e–g), we reasoned that PAA endothelium derives from *nkx2.5*$^{+}$ progenitors located in the classically defined heart-forming region, a population long considered to adopt cell fates within the heart exclusively[5,6,10]. We tested this hypothesis by employing two complementary lineage tracing strategies. First, using tamoxifen-inducible Cre/loxP lineage tracing, we transiently induced Cre activity in *nkx2.5*$^{+}$ cells for two hours during heart field stages (Supplementary Fig. 3j) and identified their derivatives

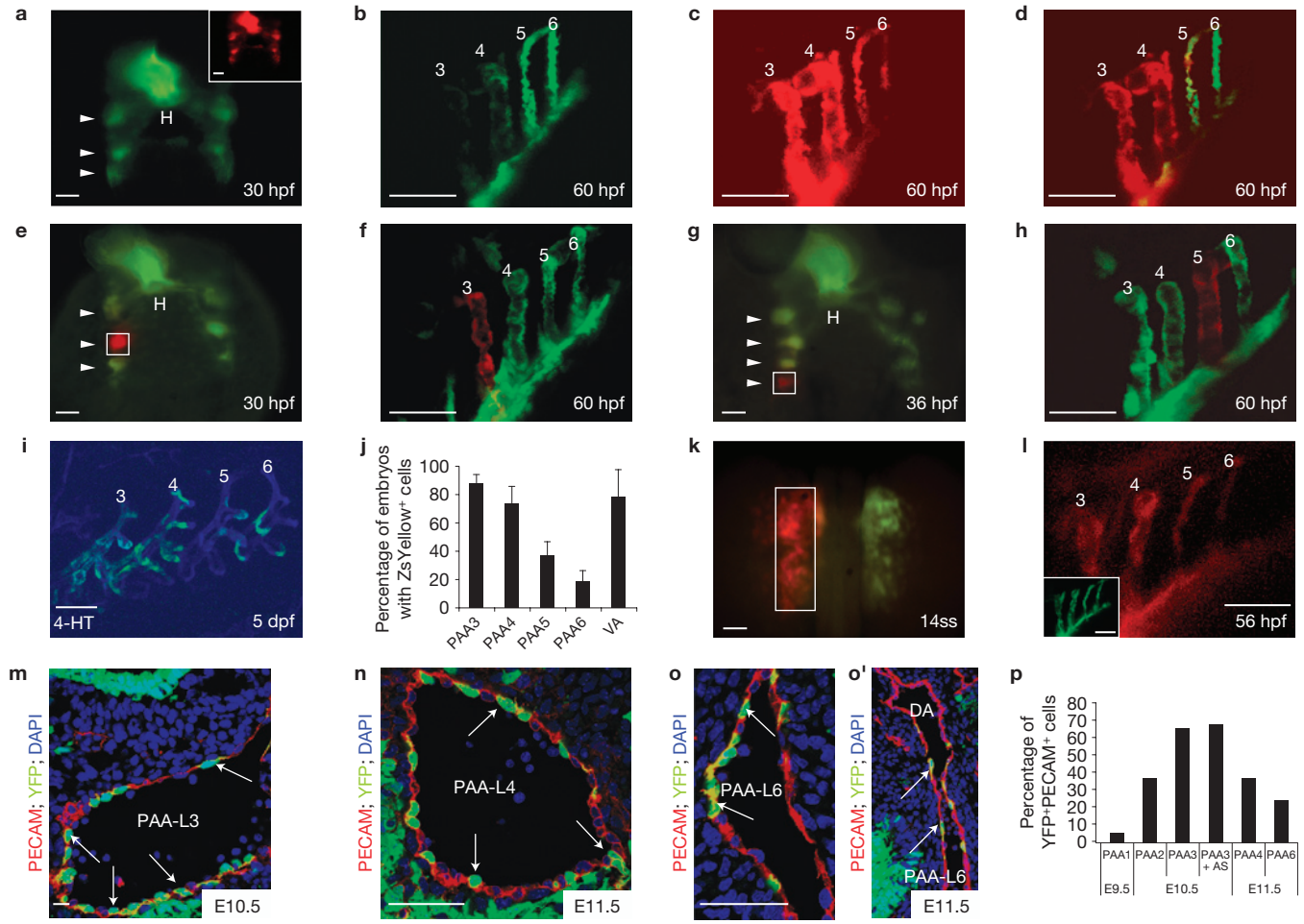

Figure 2 *nkx2.5*$^{+}$ progenitors give rise to PAA endothelium in zebrafish and mouse. (**a**–**d**) A *Tg(nkx2.5:kaede)* embryo at 30 hpf before (green) and after (red, inset) pan-photoconversion ($n = 3$). Arrowheads highlight kaede^{+} pharyngeal clusters. At 60 hpf, embryos were imaged in the green (**b**) and red (**c**) channels, and these images were then merged (**d**). (**e**–**h**) Localized kaede photoconversion of cluster 2 (**e**, white square, $n = 2$) or 4 (**g**, white square, $n = 2$) at the indicated developmental stages. Merged red and green images of the PAAs in the same embryos at 60 hpf are shown in **f**,**h**. (**i**) ZsYellow reporter fluorescence in PAAs 3–6 at 5 days post-fertilization in a *Tg(nkx2.5:CreER*^{T2}*)*; *Tg(kdrl:CSY)* embryo treated with 4-HT from 10–13 hpf. (**j**) Graph showing the average percentages of embryos with ZsYellow^{+} reporter fluorescence in each PAA and the ventral aorta (VA) across four experimental replicates ($n = 160$). Error bars indicate standard deviation. (**k**) Left anterior lateral plate mesoderm (ALPM) of a *Tg(nkx2.5:kaede)* embryo photoconverted (white rectangle) at the 14-somite stage and subsequently imaged in the red (**l**) and green channels (inset) ($n = 5$). (**m**–**o'**) *Nkx2-5*^{IRESCre}; *ROSA*^{YFP} embryos co-stained with PECAM1 (red) and DAPI (blue). Arrows indicate YFP^{+}/PECAM^{+} lineage-traced endothelial cells. (**o'**) Left PAA 6 junction with dorsal aorta. (**p**) Graph depicting the average percentage of endothelial cells (PECAM1^{+}) co-expressing YFP within each PAA. Cells counted across two embryos: E9.5 (PAA 1, $n = 244$), E10.5 (PAA 2, $n = 216$; PAA 3, $n = 1357$; PAA3 + aortic sac, $n = 642$) and E11.5 (PAAs 4, $n = 511$ and 6, $n = 649$). Dorsal views, anterior up (**a**,**e**,**g**,**k**); lateral views, anterior left (**b**–**d**,**f**,**h**,**i**,**l**). Scale bars, 50 μm. ss, somite stage; hpf, hours post-fertilization; dpf, days post-fertilization; H, heart; AS, aortic sac; DA, dorsal aorta; PAA number and left (L) and right (R) designations indicated.

using endothelial restricted (*Tg(kdrl:CSY)*) (ref. 7) or ubiquitous (*Tg(ubi:Switch)*) (ref. 11) Cre-responsive colour-switching reporters. Remarkably, we observed scattered reporter labelling of endothelial cells within PAAs 3–6 and the ventral aorta (Fig. 2i,j and Supplementary Fig. 3k–n). Most animals exhibited reporter fluorescence in PAAs 3 and 4 with lower percentages reporting fluorescence in PAAs 5 and 6 (Fig. 2j and Supplementary Fig. 3o).

In a complementary approach, we photoconverted kaede protein unilaterally in left-side *nkx2.5*$^{+}$ heart field progenitors and observed red fluorescence throughout left-side PAAs 3 and 4 with a markedly weaker signal in caudal PAAs 5 and 6 (Fig. 2k,l). As an internal control, PAAs residing contralaterally failed to express red fluorescence (Supplementary Fig. 3d–f). Furthermore, pan-photoconversion of *nkx2.5*$^{+}$ heart field cells labelled not only the heart tube, but the three pharyngeal clusters and scattered posterior cells present at 30 hpf (Supplementary Fig. 3g–i). Taken together, these data from kaede photoconversion and Cre/loxP lineage tracing demonstrate that *nkx2.5*$^{+}$ progenitors residing in the zebrafish heart field give rise to PAA endothelium. Further, the decline in labelling efficiency observed in PAAs 5 and 6 supports our previous observation that these caudal vessels derive from progenitor cells that initiate *nkx2.5* expression in the ALPM as well as those specified subsequently in pharyngeal mesoderm (Fig. 2a–h).

PAA establishment seems qualitatively similar across vertebrate species as each PAA forms in a craniocaudal sequence[12,13] through the assembly of nascent angioblasts into discrete vessels[3,4]. Although

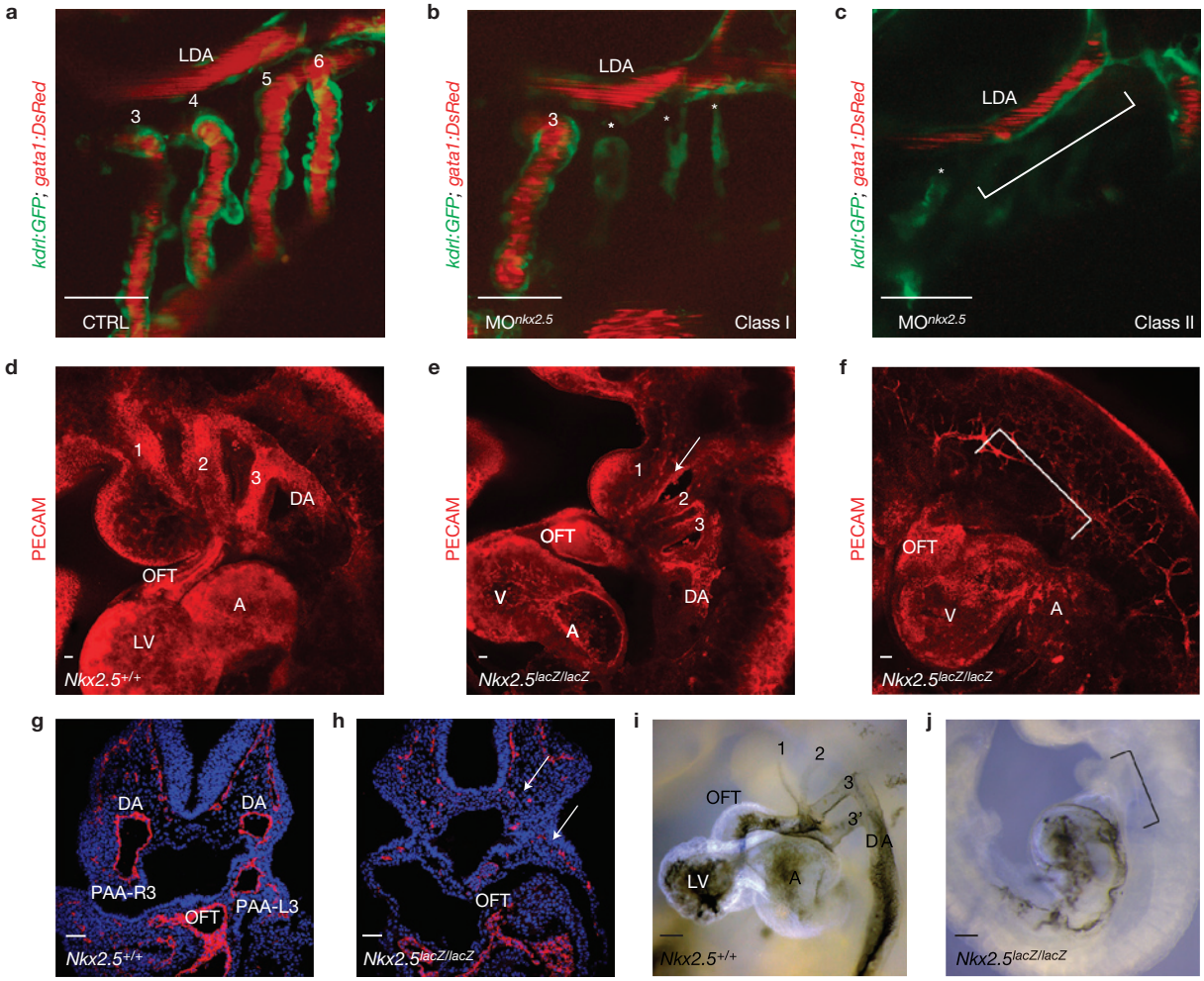

Figure 3 Nkx2.5 is required for vertebrate PAA formation. (**a**–**c**) *Tg(kdrl:GFP)*; *Tg(gata1:DsRed)* zebrafish embryos with green endothelial cells and red erythrocytes at 60 hpf. (**a**) A control (CTRL) embryo with patent PAAs 3–6 and LDA ($n = 60$ from 60). (**b**) A class I *nkx2.5* morphant ($MO^{nkx2.5}$) in which one (shown) or two PAAs support blood flow. Asterisks label malformed PAAs ($n = 88$ from 116). (**c**) Class II *nkx2.5* morphant lacking patent PAAs (bracket, $n = 22$ from 116). (**d**–**f**) Whole-mount control (**d**) or *Nkx2-5*-null (**e**,**f**) mouse embryos stained for PECAM1 (red) at E9.5 ($n = 5$ per group). *Nkx2-5*-null embryos exhibited disrupted PAAs 1–3 with residual isolated endothelial cells (arrow, **e**) or a complete absence of PAAs altogether (bracket, **f**). (**g**,**h**) Sections through control and *Nkx2-5*-null embryos stained with PECAM (red) and DAPI (blue). Arrow shows residual endothelial cells (**h**). (**i**,**j**) Ink injections in control and *Nkx2-5*-null animals at E9.5 ($n = 5$ per group). The bracket in **j** indicates absence of flow through the mutant outflow tracts. Lateral views, anterior left (**a**–**c**); lateral views, anterior up (**d**–**f**, **i**,**j**); coronal sections (**g**,**h**). Scale bars, 50 μm. LDA, lateral dorsal aorta; DA, dorsal aorta; OFT, outflow tract; LV, left ventricle; A, atrium; V, ventricle; PAA number and left (L) and right (R) designations indicated.

the progenitor source of these angioblasts had not been defined previously, a Cre recombinase-based lineage tracing study noted descendants of *Nkx2-5*-expressing cells in endocardium as well as putative endothelial cells scattered throughout the first pharyngeal arch[14]. Nonetheless, PAAs were not systematically examined, and in the absence of co-labelling studies and high-resolution imaging, the molecular identity of the traced cells remains unclear. To conclusively determine whether PAA endothelium in the mouse derives from $Nkx2\text{-}5^{+}$ progenitors, we performed Cre/loxP lineage tracing using the previously characterized $Nkx2\text{-}5^{IRESCre}$ driver[14] with the *Z/EG* (ref. 15) or $ROSA^{YFP}$ (ref. 16) reporters followed by immunostaining with the endothelial cell marker PECAM1. As anticipated, robust reporter expression was observed in the myocardium and endocardium of the heart[14] (Supplementary Fig. 3p,q). Strikingly, reporter fluorescence at embryonic day (E)9.5 and E10.5 co-localized with PECAM1 in PAAs 1 and 2, respectively (Fig. 2p and Supplementary Fig. 3r,s). At later stages, reporter fluorescence was also observed in PAAs 3, 4 and 6 (Fig. 2m–p and Supplementary Fig. 3t), the embryonic vessels that generate critical segments of the postnatal carotid arteries, right subclavian artery and aorta, and pulmonary arteries, respectively[12,17]. Rare overlap was also observed in the dorsal aorta endothelium at the sites of PAA attachment (Fig. 2o'). These findings highlight the evolutionary conservation of PAA endothelial cell derivation from an $Nkx2\text{-}5^{+}$ source in mammals.

To assess the requirement for *nkx2.5* during PAA establishment in zebrafish, we employed a previously validated anti-sense morpholino[18] to suppress Nkx2.5 function (Supplementary Fig. 4a,b). Whereas control embryos exhibited strong blood flow through PAAs 3–6 (Fig. 3a), *nkx2.5* morphants exhibited either a reduction in PAA number (class I; Fig. 3b) or an absence of PAAs altogether (class II; Fig. 3c). Importantly, PAA1, which establishes the initial circulatory loop in

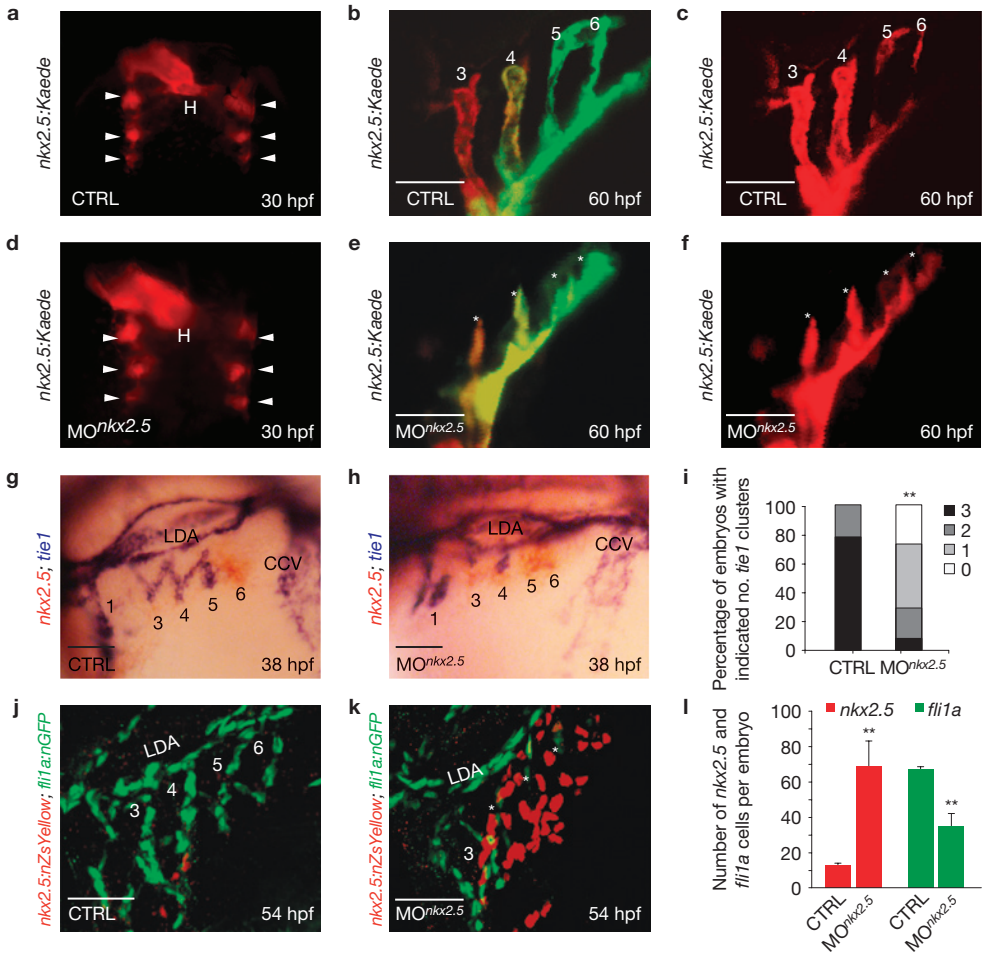

Figure 4 Nkx2.5 is required for PAA progenitor cell differentiation. (**a**–**f**) Control (CTRL; $n=3$) and *nkx2.5* morphant ($n=5$) *Tg(nkx2.5:kaede)* embryos were pan-photoconverted at 30 hpf (**a**,**d**). Arrowheads show kaede^{+} pharyngeal clusters. At 60 hpf, embryos were imaged in red and green channels with red (**c**,**f**) and merged (**b**,**e**) images are shown. Asterisks (**e**,**f**) mark abnormal PAAs 3–6 in *nkx2.5* morphant embryos. (**g**,**h**) *nkx2.5* (red) and *tie1* (blue) transcripts evaluated by double *in situ* hybridization in control (**g**) and morphant (**h**) embryos. (**i**) Quantification of *tie1*$^{+}$ clusters in control ($n=95$) and *nkx2.5* morphant ($n=42$) embryos across three experimental replicates; two-tailed *t*-test $^{**}P=0.0001$. (**j**,**k**) Control and nkx2.5 morphant *Tg(nkx2.5:nZsYellow); Tg(fli1a:nEGFP)* embryos showing *nkx2.5*$^{+}$ PAA progenitors (red) and *fli1a*$^{+}$ endothelial cells (green) detected by immunohistochemistry. (**l**) Quantification of *nkx2.5*$^{+}$ and *fli1a*$^{+}$ cells in control ($n=4$) and *nkx2.5* morphant ($n=4$) embryos; error bars indicate standard deviation, two-tailed *t*-test *nkx2.5* $^{**}P=0.0073$, *fli1a* $^{**}P=0.0008$ across three independent experiments. Scale bars, 50 μm. LDA, lateral dorsal aorta; CCV, common cardinal vein. Dorsal views, anterior up (**a**,**d**); lateral views, anterior left (**b**,**c**,**e**,**f**,**g**,**h**,**j**,**k**); PAA numbers indicated.

zebrafish, develops much earlier in an *nkx2.5*-independent manner[13,19] (Fig. 1p). As such, both morphant classes maintained robust blood flow through the remaining vasculature, reducing the likelihood that haemodynamic alterations caused the observed phenotype. Consistent with this idea, PAA vasculogenesis occurs normally in *silent heart* mutants that completely lack heart function and blood flow[20].

Compared with control mouse embryos that exhibited well-formed PAAs 1–3 at E9.5 (Fig. 3d), *Nkx2-5*$^{lacZ/lacZ}$-null animals exhibited either disrupted PAAs with residual mis-patterned endothelial cells (Fig. 3e) or a complete absence of PAAs altogether (Fig. 3f and Supplementary Fig. 4g–i). Whereas ink injections in wild-type embryos revealed patent cardiac outflow tracts with prominent forward flow into the paired PAA3 vessels (Fig. 3i), the outflow tracts in *Nkx2-5*$^{lacZ/lacZ}$ mutants ended in a blind sac (Fig. 3j). These data demonstrate a previously unappreciated requirement for Nkx2-5 in PAA establishment that is conserved from zebrafish to mammals.

To elucidate the cellular mechanism underlying the PAA defect in Nkx2.5-deficient zebrafish, we evaluated *nkx2.5* morphants for PAA progenitor cell specification and differentiation. Using a transgenic strain that highlights *nkx2.5*$^{+}$ nuclei, we documented equivalent numbers of *nkx2.5*$^{+}$ progenitors in control and morphant heart fields (Supplementary Fig. 4j–l), indicating proper specification. Examination of fluorescence in morpholino-injected *Tg(nkx2.5:kaede)* embryos revealed that PAA progenitor cells also clustered normally by 30 hpf (Fig. 4a,d). Photoconversion of kaede expressed within morphant clusters revealed that they were maintained properly in the pharynx, but failed to form organized vessels, suggesting that Nkx2.5 is required specifically for PAA vasculogenesis (Fig. 4b,c,e,f). Next, we evaluated morphants for *nkx2.5* and *tie1* expression in pharyngeal clusters undergoing endothelial differentiation. In control embryos, we observed differentiated *tie1*$^{+}$ clusters that had successfully downregulated *nkx2.5* (Fig. 4g,i). In contrast, morphant embryos

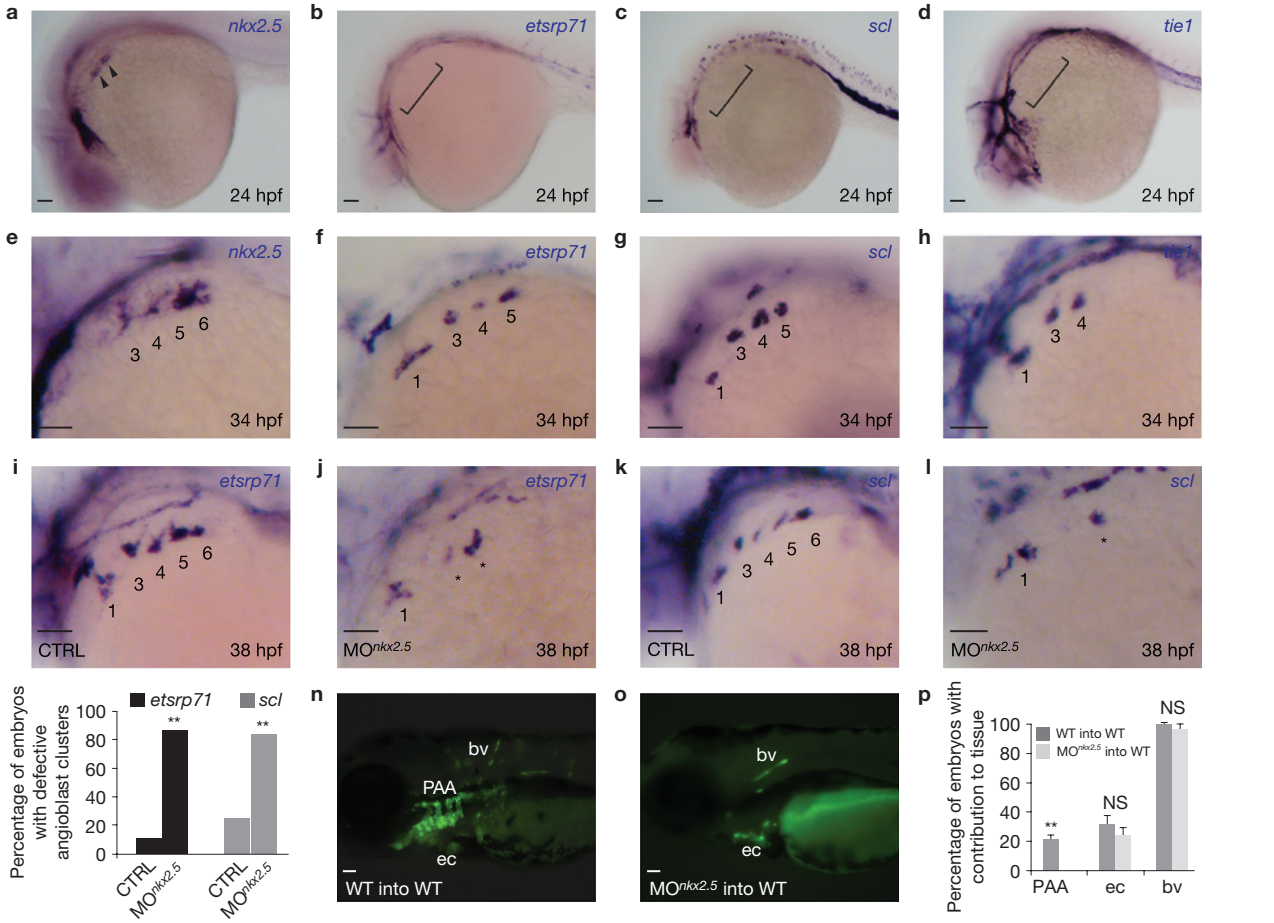

Figure 5 Cell-autonomous requirement for Nkx2.5 in promoting the PAA progenitor to angioblast transition. (**a**–**h**) *In situ* hybridization analysis of *nkx2.5* (**a**,**e**), *etsrp71* (**b**,**f**),*scl* (**c**,**g**), and *tie1* (**d**,**h**) at 24 (**a**–**d**) and 34 (**e**–**h**) hpf. **i**–**l** *etsrp* (**i**,**j**) and *scl* (**k**,**l**) transcripts evaluated by *in situ* hybridization in control (CTRL; **i**,**k**) and *nkx2.5* morphant ($MO^{nkx2.5}$; **j**,**l**) embryos; asterisks mark abnormal PAAs 3–6. (**m**) Quantification of embryos with defective angioblast clusters. *etsrp* CTRL $n = 61$, $MO^{nkx2.5}$ $n = 53$, two-tailed *t*-test $^{**}P = 0.001$ across two independent experiments; *scl* CTRL $n = 106$, $MO^{nkx2.5}$ $n = 116$, two-tailed *t*-test $^{**}P = 0.001$ across two independent experiments. **n**–**p**, Wild-type (WT; **n**) and $MO^{nkx2.5}$ (**o**) donor-derived GFP^+ PAA endothelium in unlabelled wild-type hosts. (**p**) Quantification of host embryos showing GFP^+ donor cells from wild-type ($n = 208$) or $MO^{nkx2.5}$ ($n = 86$) embryos in the PAAs, endocardium (ec) and body vasculature (bv). Fisher's exact test, PAA two tailed $^{**}P = 0.0001$; endocardium, two-tailed $P = 0.3239$ (not significant, NS); body vasculature, two-tailed $P = 0.2710$, across four independent experiments. Scale bars, 50 μm. Lateral views, anterior left; PAA islands indicated (**a**–**l**); $n > 20$ embryos per group (**a**–**h**); error bars indicate standard deviation (**m**,**p**).

exhibited persistent expression of *nkx2.5* in clusters that failed to appropriately upregulate *tie1* (Fig. 4h,i), a phenotype that can be rescued by co-injection of full-length zebrafish *nkx2.5* messenger RNA (Supplementary Fig. 4c–f). Using a double transgenic strain expressing unique fluorescent proteins in the nuclei of either PAA progenitors (red) or endothelial cells (green), we quantified the high degree to which PAA progenitors accumulate at the expense of endothelial cell differentiation in morphant embryos (Fig. 4j–l). Together, these data reveal that Nkx2.5 is dispensable for PAA progenitor specification and maintenance but essential for endothelial differentiation.

To identify potential downstream mediators of *nkx2.5*-dependent endothelial cell differentiation, we examined pharyngeal mesoderm for the expression of two transcription factors, *etsrp71* and *scl*, shown previously to be associated with early specification of the angioblast lineage[21]. At 24 hpf, only *nkx2.5* transcripts were visible in pharyngeal clusters (Fig. 5a–d). At 34 hpf, however, we observed four $nkx2.5^+$ clusters (Fig. 5e), three $etsrp71^+$, scl^+ clusters (Fig. 5f,g) and two $tie1^+$ clusters (Fig. 5h), indicating that *etsrp71* and *scl* transcripts appear subsequent to *nkx2.5* but before *tie1* in each cluster. Further, we learned that knocking down *nkx2.5* inhibits the expression of *etsrp71* and *scl* in PAA progenitors (Fig. 5i–m), demonstrating that *nkx2.5* function is required for initiating the angioblast program.

To determine whether Nkx2.5 is required cell autonomously for PAA vasculogenesis, we generated chimaeric embryos through blastula transplantation. Wild-type or *nkx2.5*- deficient donor cells carrying an endothelial transgene (*Tg(kdrl:GFP)*) were transplanted into unlabelled wild-type blastula hosts. Both control and *nkx2.5*-deficient donor cells contributed equally to the body vasculature and endocardium (Fig. 5n–p). However, *nkx2.5*-deficient donor cells failed to contribute to PAA endothelium (Fig. 5o,p), demonstrating that Nkx2.5 is required cell autonomously in PAA progenitors for endothelial differentiation. Moreover, because the haemodynamic environments of the host embryos were unaltered, these findings further solidify the conclusion that Nkx2.5 plays a primary role in PAA establishment.

Our observations support a model (Supplementary Fig. 1) in which *nkx2.5*$^{+}$ PAA progenitors segregate from cardiac precursors in the heart field and condense into clusters concomitant with pharyngeal segmentation[22]. Clusters 2 and 3 give rise to PAAs 3 and 4, respectively. Further, a small number of *nkx2.5*-expressing heart field progenitors migrate to arches 5 and 6 where naive mesodermal cells initiate *nkx2.5* expression in the pharynx.

Our findings also highlight a previously unknown and conserved role for Nkx2.5 in blood vessel development. This pro-vasculogenic function of Nkx2.5 was largely unanticipated because previous work demonstrated that misexpression of Nkx2.5 repressed *scl*$^{+}$ haemangioblast fates in a region of the ALPM anterior to the heart field[23] (Supplementary Fig. 5a,b). However, overexpression of *nkx2.5* did not reduce or expand *tie1*$^{+}$ PAA endothelial cluster formation in the pharynx (Supplementary Fig. 5c–e), highlighting context-dependent roles for Nkx2.5 in angioblast specification. These data also demonstrate that PAA progenitor cell differentiation to the endothelial lineage does not require downregulation of *nkx2.5* that otherwise occurs naturally (Fig. 1i–p). Furthermore, FGF signalling was shown to promote ALPM haemangioblast fates at the expense of cardiac fates[23] (Supplementary Fig. 5f,g). Inhibition of FGF signalling did not alter PAA progenitor cluster formation or endothelial differentiation, indicating a dispensable role for FGF signalling during these stages of PAA morphogenesis (Supplementary Fig. 5h–l). Together, these findings demonstrate that Nkx2.5 actively represses angioblast differentiation early in the ALPM and is required, but not sufficient, for angioblast differentiation later in the pharynx. Although Nkx2.5 targets have been identified within the myocardium[24] and endocardium[25], the *cis*-acting regulatory sequences that are directly activated or repressed by Nkx2.5 during PAA angioblast emergence remain unidentified.

Although *nkx2.5* expression in PAA progenitors commences by 14 hpf, Nkx2.5 function is not required until approximately 30 hpf to activate the PAA vasculogenic program (Figs 1m–p and 4). This delay suggests that *nkx2.5*$^{+}$ PAA progenitors integrate a stage- and/or location-specific external cue to cooperatively promote the angioblast fate. However, following endothelial program initiation, *nkx2.5* expression downregulates, indicating a specific requirement in promoting the progenitor to angioblast transition. In zebrafish, each PAA wholly derives from *nkx2.5*$^{+}$ cells, and Nkx2.5 is essential cell autonomously for initiating PAA morphogenesis. However, our lineage tracing and knockout studies in the mouse highlight the possibility that more than one progenitor population contributes to PAA endothelium, as suggested for endocardium[26,27]. Nonetheless, our work overwhelmingly supports a conserved role for Nkx2-5 in PAA development across vertebrate species. Intriguingly, NKX2.5 mutations in humans can lead to interrupted aortic arch type B (ref. 28), a great vessel malformation involving left PAA4. Although the etiology of this congenital heart defect has been attributed to abnormal regression of left PAA4 (ref. 29), interrupted aortic arch type B might also arise from defects in PAA establishment. □

METHODS

Methods and any associated references are available in the online version of the paper.

Note: Supplementary Information is available in the online version of the paper

ACKNOWLEDGEMENTS

We are grateful to S. Paskaradevan and I. Scott (University of Toronto, USA) for their training in blastula transplantation. We thank C. Kinney for creating Supplementary Fig. 1; P. Obregon and T. Cashman for technical assistance in generating the *Tg(nkx2.5:kaede)* and *Tg(nkx2.5:nZsYellow)* transgenic lines, respectively; W. Goessling (Harvard Medical School, USA) for providing *Tg(sox17:GFP)* fish; T. North, and L. Zon (Harvard Medical School, USA) for providing *Tg(kdrl:GFP)* fish; I. Drummond (Massachusetts General Hospital, USA) for providing *bon*^{m425} fish; B. Barut (Harvard Medical School, USA) and L. Zon for providing bacterial artificial chromosomes; T. Evans (Weill Cornell Medical College, USA) for providing *nkx2.5* plasmid for probe generation; G. Wilkinson (Medical College of Wisconsin, USA) and S. Sumanas (Cincinnati Children's Hospital Medical Center, USA) for providing *etsrp71* plasmid for probe generation; and the MGH Nephrology Division for access to their confocal microscopy facilities. We thank A. Vasilyev for assistance with confocal microscopy. N.P.L was supported by the Harvard Stem Cell Institute Training Grant (5HL087735) and a National Research Service Award (1F32HL 112579) from the National Heart, Lung and Blood Institute (NHLBI). B.G-A. was financially supported by an American Heart Association (AHA) Post-Doctoral Fellowship (10POST4170037). K.R.N. is financially supported by a National Research Service Award (5F32HL110627) from the National Heart, Lung and Blood Institute (NHLBI). R.P.H. is supported by grants from the National Health and Medical Research Council of Australia (NHMRC; 573732, 573703), Atlantic Philanthropies (19131) and National Heart Foundation of Australia (G08S3718). R.P.H. holds an NHMRC Australia Fellowship (573705). This work was financially supported by awards from the National Heart Lung and Blood Institute (5R01HL096816), American Heart Association (Grant in Aid no. 10GRNT4270021), and Harvard Stem Cell Institute (Seed Grant) to C.G.B. and the National Heart Lung and Blood Institute (5R01HL111179), the March of Dimes Foundation (FY12-467), and the Harvard Stem Cell Institute (Seed Grant and Young Investigator Award) to C.E.B. R.P.H. dedicates this work to Irene Myrtle Harvey, 1923–2013, from whom scholarship and inspiration were drawn.

AUTHOR CONTRIBUTIONS

N.P-L. designed and performed the zebrafish experiments, analysed data and co-wrote the paper; R.S. designed, performed and analysed the mouse experiments, and co-wrote the paper; C.G.B. and B.G-A. created the *Tg(nkx2.5:CreER*^{T2}*)* and *Tg(nkx2.5:nZsYellow)* lines; K.R.N., E.O.L. and L.J. performed and analysed zebrafish experiments; R.P.H. analysed data, designed experiments and co-wrote the paper; C.G.B. and C.E.B. initiated and directed the study, analysed data, and co-wrote the paper with input from all authors.

COMPETING FINANCIAL INTERESTS

The authors declare no competing financial interests.

Published online at www.nature.com/doifinder/10.1038/ncb2862
Reprints and permissions information is available online at www.nature.com/reprints

1. Congdon, E. D. Transformation of the aortic arch system during the development of the human embryo. *Contrib. Embryol.* **68,** 49–110 (1922).
2. Moore, K. L. & Persaud, T. V. N. *The Developing Human: Clinically Oriented Embryology* 5th edn (Saunders, 1993).
3. Anderson, M. J., Pham, V. N., Vogel, A. M., Weinstein, B. M. & Roman, B. L. Loss of unc45a precipitates arteriovenous shunting in the aortic arches. *Dev. Biol.* **318,** 258–267 (2008).
4. Li, P., Pashmforoush, M. & Sucov, H. M. Mesodermal retinoic acid signaling regulates endothelial cell coalescence in caudal pharyngeal arch artery vasculogenesis. *Dev. Biol.* **361,** 116–124 (2012).
5. Ma, Q., Zhou, B. & Pu, W. T. Reassessment of Isl1 and Nkx2-5 cardiac fate maps using a Gata4-based reporter of Cre activity. *Dev. Biol.* **323,** 98–104 (2008).
6. Schoenebeck, J. J., Keegan, B. R. & Yelon, D. Vessel and blood specification override cardiac potential in anterior mesoderm. *Dev. Cell* **13,** 254–267 (2007).
7. Zhou, Y. *et al.* Latent TGF-beta binding protein 3 identifies a second heart field in zebrafish. *Nature* **474,** 645–648 (2011).
8. Serbedzija, G. N., Chen, J. N. & Fishman, M. C. Regulation in the heart field of zebrafish. *Development* **125,** 1095–1101 (1998).
9. Guner-Ataman, B. *et al.* Zebrafish second heart field development relies on progenitor specification in anterior lateral plate mesoderm and nkx2.5 function. *Development* **140,** 1353–1363 (2013).
10. Hami, D., Grimes, A. C., Tsai, H. J. & Kirby, M. L. Zebrafish cardiac development requires a conserved secondary heart field. *Development* **138,** 2389–2398 (2011).
11. Mosimann, C. *et al.* Ubiquitous transgene expression and Cre-based recombination driven by the ubiquitin promoter in zebrafish. *Development* **138,** 169–177 (2011).
12. Hiruma, T., Nakajima, Y. & Nakamura, H. Development of pharyngeal arch arteries in early mouse embryo. *J. Anat.* **201,** 15–29 (2002).

13. Isogai, S., Horiguchi, M. & Weinstein, B. M. The vascular anatomy of the developing zebrafish: an atlas of embryonic and early larval development. *Dev. Biol.* **230,** 278–301 (2001).
14. Stanley, E. G. *et al.* Efficient Cre-mediated deletion in cardiac progenitor cells conferred by a 3'UTR-ires-Cre allele of the homeobox gene Nkx2-5. *Int. J. Dev. Biol.* **46,** 431–439 (2002).
15. Novak, A., Guo, C., Yang, W., Nagy, A. & Lobe, C. G. Z/EG, a double reporter mouse line that expresses enhanced green fluorescent protein upon Cre-mediated excision. *Genesis* **28,** 147–155 (2000).
16. Srinivas, S. *et al.* Cre reporter strains produced by targeted insertion of EYFP and ECFP into the ROSA26 locus. *BMC Dev. Biol.* **1,** 1478 (2001).
17. Kaufman, M. H. & Bard, J. B. L. *The Anatomical Basis of Mouse Development* 1st edn (Academic, 1999).
18. Targoff, K. L., Schell, T. & Yelon, D. Nkx genes regulate heart tube extension and exert differential effects on ventricular and atrial cell number. *Dev. Biol.* **322,** 314–321 (2008).
19. Westerfield, M. *The Zebrafish Book. A Guide for the Laboratory Use of Zebrafish (Danio rerio)* 4th edn (Univ. Oregon Press, 2000).
20. Nicoli, S. *et al.* MicroRNA-mediated integration of haemodynamics and Vegf signalling during angiogenesis. *Nature* **464,** 1196–1200 (2010).
21. Sumanas, S. & Lin, S. Ets1-related protein is a key regulator of vasculogenesis in zebrafish. *PLoS Biol.* **4,** 483–494 (2006).
22. Schilling, T. F. & Kimmel, C. B. Segment and cell type lineage restrictions during pharyngeal arch development in the zebrafish embryo. *Development* **120,** 483–494 (1994).
23. Simoes, F. C., Peterkin, T. & Patient, R. Fgf differentially controls cross-antagonism between cardiac and haemangioblast regulators. *Development* **138,** 3235–3245 (2011).
24. He, A., Kong, S. W., Ma, Q. & Pu, W. T. Co-occupancy by multiple cardiac transcription factors identifies transcriptional enhancers active in heart. *Proc. Natl Acad. Sci. USA* **108,** 5632–5637 (2011).
25. Ferdous, A. *et al.* Nkx2-5 transactivates the Ets-related protein 71 gene and specifies an endothelial/endocardial fate in the developing embryo. *Proc. Natl Acad. Sci. USA* **106,** 814–819 (2009).
26. Harris, I. S. & Black, B. L. Development of the endocardium. *Pediatr. Cardiol.* **31,** 391–399 (2010).
27. Milgrom-Hoffman, M. *et al.* The heart endocardium is derived from vascular endothelial progenitors. *Development* **138,** 4777–4787 (2011).
28. McElhinney, D. B., Geiger, E., Blinder, J., Benson, D. W. & Goldmuntz, E. NKX2.5 mutations in patients with congenital heart disease. *J. Am. College Cardiol.* **42,** 1650–1655 (2003).
29. Stoller, J. Z. & Epstein, J. A. Cardiac neural crest. *Semin. Cell Dev. Biol.* **16,** 704–715 (2005).

DOI: 10.1038/ncb2862

METHODS

Zebrafish husbandry and strains. Zebrafish were grown and maintained according to protocols approved by the Massachusetts General Hospital Institutional Animal Care and Use Committee. *Tg(nkx2.5: ZsYellow)*^{fb7} (ref. 9); *Tg(kdrl:CSY)*^{fb3} (ref. 7) double transgenic embryos were imaged live by confocal analysis to confirm the endothelial nature of the ZsYellow^{+} PAAs in the *Tg(nkx2.5:ZsYellow)*^{fb7} embryos. As Cre recombinase was not present, all endothelial cells in these embryos are marked by blue fluorescence. *bonnie and clyde* (*bon*^{m425}; ref. 30) was crossed into the *Tg(nkx2.5:ZsYellow)*^{fb7} background and genotyped as described previously[30]. *Tg(nkx2.5:ZsYellow)*^{fb7}*;Tg(sox17:GFP)*^{s870} (ref. 31) double transgenic embryos were used to mark *nkx2.5* and endodermal populations, respectively. Previously characterized driver *Tg(nkx2.5:CreER*^{T2}*)*^{fb8} (ref. 9) and reporter *Tg(kdrl:LOXP–AmCyan–LOXP–ZsYellow)*^{fb3} (ref. 7) or *Tg(ubi:loxP–EGFP–loxP–mCherry)*^{cz1701} (*Tg(ubi:Switch)*) (ref. 11) transgenic animals were used for Cre/Lox lineage tracing. *Tg(nkx2.5:kaede)*^{fb9} (ref. 9) embryos were used for fate-mapping. *Tg(kdrl:GFP)*^{la116} (ref. 32); *Tg(gata1:DsRed)*^{sd2} (ref. 33) double transgenic embryos were used to visualize endothelium and blood flow through the PAAs. *Tg(nkx2.5:nZsYellow); Tg(fli1a:nEGFP)*^{y7} (ref. 34) double transgenic embryos were used to concurrently enumerate endothelial and *nkx2.5* cells, respectively. Cell nuclei were counted in *Z*-stack confocal images using ImageJ software[35]. Cells from *Tg(kdrl:GFP)*^{la116} (ref. 32) donor embryos were transplanted into wild-type TuAB hosts for mosaic analysis. *Tg(cmlc2:EGFP)*^{f1} (ref. 36) embryos were used to assess the FGF inhibitor treatment. Unless specified otherwise, live embryos were incubated in E3 embryo media[19] at 28.5 °C and anaesthetized in embryo media containing 0.4% tricaine (ethyl 3-aminobenzoate methanesulphonate, MS222; Sigma).

Generation of the *TgBAC(-36nkx2.5:H2B-ZsYellow)* (*Tg(nkx2.5:nZsYellow)*) transgenic strain. A bacterial artificial chromosome (BAC; DKEY-9I15) with ~36 kilobases (kb) and ~194 kb upstream and downstream, respectively, of the first *nkx2.5* exon was obtained. BAC recombineering was used to replace the first exon coding sequence for Nkx2.5 with that of a nuclear ZsYellow protein (H2B–ZsYellow) as described previously[7]. The BAC insert was surrounded by ISceI sites through two additional rounds of recombineering. For germline transmission, the modified BAC was co-injected with ISceI meganuclease. Further details are available on request.

Zebrafish whole-mount *in situ* hybridization. Single and double riboprobe whole-mount *in situ* hybridizations were performed in glass vials essentially as described previously[37,38] using digoxygenin- or fluorescein-labelled anti-sense RNA probes against *nkx2.5* and *tie1*. Probes were synthesized using a DIG RNA Labelling Kit (SP6/T7; Roche Applied Science). Blue (NBT/BCIP) and red (INT/BCIP) chromogenic substrates were used (Roche Applied Science).

Zebrafish immunohistochemistry. Manipulations were performed at room temperature unless otherwise stated[7]. Embryos were fixed overnight at 4 °C in 80% methanol/20% dimethylsulphoxide, dehydrated in a methanol series, and stored in 100% methanol at −20 °C. Embryos were rehydrated to 1XPBS/0.5% Triton X-100 (PBSTx) and blocked with PBSTx/1% BSA/0.1% dimethylsulphoxide for 3 h. Embryos were incubated with primary antibodies diluted in blocking solution overnight at 4 °C. Embryos were washed 6 × 15 min in PBSTx and incubated with secondary antibodies diluted in blocking solution for two hours. Secondary antibodies were removed by washing with PBSTx for 3 × 30 min before storage at 4 °C in PBSTx. Primary antibodies specific for GFP (B-2 mouse monoclonal; Santa Cruz Biotechnology, catalogue number sc-9996) and ZsYellow (anti-RCFP rabbit polyclonal antibody; Clontech, catalogue number 632475) were incubated at 1:50 dilution. Secondary antibodies (Alexa Fluor 488 goat α-mouse IgG, Alexa Fluor 555 goat α-rabbit IgG (Invitrogen Carlsbad)) were used at dilutions of 1:200.

Zebrafish lineage tracing. Driver *Tg(nkx2.5:CreER*^{T2}*)*^{fb8} and reporter *Tg(kdrl:LOXP–AmCyan–LOXP–ZsYellow)*^{fb3} or *Tg(ubi:loxP–EGFP–loxP–mCherry)*^{cz1701} transgenic animals were used for Cre/loxP lineage tracing as described previously[9,11]. To induce Cre activity in *Tg(nkx2.5:CreER*^{T2}*)*-expressing embryos, tailbud staged (10 hpf) embryos were incubated in E3 medium with 10 μM 4-hydroxytamoxifen (4-HT, H7904; Sigma) or ethanol carrier control. Embryos were kept in the dark until the 8-somite stage (~13 hpf) and washed with 500 ml of fresh E3 medium to remove all traces of 4-HT. The embryos were allowed to develop in fresh E3 medium until 5 days post-fertilization, at which point they were evaluated for yellow or red reporter fluorescence expression. Embryos with colour-switch events were used to determine the percentage of embryos with reporter fluorescence in each PAA and in the ventral aorta.

Zebrafish kaede photoconversion. Pan-kaede photoconversion was achieved by mounting individual *Tg(nkx2.5:kaede)*^{fb9} embryos in 0.9% lo-melt agarose in glass-bottom dishes (MatTek Corporation) and exposing kaede to fluorescent light passed through the DAPI filter on a Nikon 80i compound microscope (Nikon Instruments) using the ×10 objective until all green fluorescence was lost (approximately 3 min). Embryos were immediately imaged, removed from agarose, and raised in dark isolation until subsequent evaluation. Specific cell populations were similarly photoconverted using the 405 nm blue diode laser on a Zeiss LSM5 Pascal laser scanning microscope (Carl Zeiss MicroImaging).

Zebrafish morpholino and mRNA injections. Morpholinos were purchased from Gene Tools (Oregon). To generate MO$^{nkx2.5}$ embryos, one-cell stage embryos were injected with 1 nl of previously characterized antisense morpholino targeting *nkx2.5* splicing[18] at 3.32 ng nl^{-1}. Efficient knockdown was evaluated by PCR with reverse transcription, in which total RNA was extracted from 28-hpf control and morphant embryos using Trizol Reagent (Life Technologies). Complementary DNA was synthesized using Superscript III First Strand Synthesis System (Life Technologies). Primers F1, R1 and R2 (ref. 18) were used to amplify first-strand cDNAs for unspliced (F1/R1) or spliced (F1/R2) *nkx2.5* transcripts. Amplification of 18S ribosomal RNA (ref. 39) was used as a loading control. Specificity of the *nkx2.5* knockdown was achieved by rescue with 50 pg full-length, capped zebrafish *nkx2.5* mRNA (ref. 9), transcribed using mMessage mMachine (Invitrogen). Zebrafish *nkx2.5* mRNA (50–100 pg) was injected into one-cell stage zebrafish embryos for overexpression analysis as previously described[23], and evaluated for *tie1* and *scl* by *in situ* hybridization.

Inhibition of FGF signalling. As previously described[23,40], wild-type, *Tg(nkx2.5:ZsYellow)*^{fb7} and *Tg(cmlc2:GFP)*^{f1} zebrafish embryos were incubated in 10 μM SU5402 (Sigma), or an equivalent amount of dimethylsulphoxide, starting at the 5-somite stage and raised in the dark. *Tg(nkx2.5:ZsYellow)*^{fb7} embryos were visualized for ZsYellow fluorescence at 28 hpf, wild-type embryos were fixed for *tie1 in situ* hybridization at 34 hpf, and the hearts of *Tg(cmlc2:GFP)*^{f1} embryos were visualized at 72 hpf.

Zebrafish microscopy. Live or processed embryos were imaged on a Nikon 80i compound microscope (Nikon Instruments) with a Retiga 2000R high-speed CCD (charge-coupled device) camera (QImaging) and an NIS-Elements advanced research image acquisition and analysis system (Nikon Instruments). Confocal microscopy was performed using a Zeiss LSM5 Pascal laser scanning microscope (Carl Zeiss MicroImaging). AmCyan was excited with a 405 nm blue diode laser and imaged through a 475 nm long-pass filter. GFP was excited with a 488 nm argon laser and imaged through a 505–536 nm filter. ZsYellow protein was excited with a 514 nm argon laser and imaged through a 530 nm long-pass filter. DsRed and mCherry were excited with a 543 nm HeNe laser and imaged through a 560 nm long-pass filter. Embryos processed by *in situ* hybridization were imaged in 100% glycerol on the compound microscope using the ×4, ×10 or ×20 objectives. Live fluorescent embryos were mounted in 0.9% lo-melt agarose in glass-bottom dishes (MatTek Corporation). Live embryos imaged by confocal analysis were mounted as described and covered with embryo media containing 0.4% tricaine and imaged with the ×40 water immersion lens. Images of live embryos captured with the compound microscope were mounted in agarose as described and covered with a glass coverslip. Embryos processed by fluorescent immunohistochemistry were flat-mounted in 9:1 glycerol/PBS with 2% *N*-propyl gallate on slides with one or two layers of electrical tape containing a cut-out window, and immobilized with coverslips and images were captured by confocal analysis using the ×20 objective.

Zebrafish transplantation. *Tg(kdrl:GFP)*^{la116} donor embryos were injected with 1 nl of 5 mg ml^{-1} tetramethylrhodamine dextran (relative molecular mass 10,000, Invitrogen) as the lineage tracer and 3.32 ng nl^{-1} *nkx2.5* morpholino, as indicated. A total of 30–40 cells were removed from the animal cap of 4 hpf donor embryos and transplanted into the margin of equivalently staged wild-type host embryos. Embryos were raised individually in E2 embryo medium[41]. At 24 hpf, host embryos were evaluated for rhodamine contribution. Equivalent percentages of rhodamine^{+} cells were detected in hosts from wild-type (88%) and *nkx2.5* morphant (86%) donors, indicating that wild-type and *nkx2.5* morphant donors were equally able to contribute to host tissues. At 3 days post-fertilization, host embryos were scored for donor GFP fluorescence. Only those embryos showing donor-derived *kdrl*$^{+}$ endothelium were selected for further analysis in which we determined how many of the total number of chimaeras showed donor cell contribution to the PAAs, endocardium or blood vessels. We performed the transplant experiment 4 times and generated a total of $n = 208$ control and $n = 86$ *nkx2.5* morphant chimaeras for our

collective analyses. We averaged the results across the 4 experimental replicates and the error bars represent 1 s.d. from the mean.

Mouse husbandry and strains. Mice used in this study were bred and maintained in the Victor Chang Cardiac Research Institute BioCore facility according to the Australian Code of Practice for the Care and Use of Animals for Scientific Purposes. Intercrosses between the previously described *Nkx2-5*$^{lacZ/+}$ strain were used for generating *Nkx2-5*-null embryos[42]. For Cre lineage studies, the *Nkx2-5*^{irescre} strain[14] was crossed either with *Z/EG* (ref. 15) or *Rosa*^{YFP} (ref. 16) reporter lines.

Mouse immunostaining. Embryos were dissected in ice-cold phosphate-buffered saline (PBS) and fixed overnight in 4% paraformaldehyde (PFA) at 4 °C. Embryos were dehydrated through a series of 25, 50, 75 and 100% methanol and stored at −20 °C before staining. Whole-mount immunostaining was performed according to the previously described methods[42]. PBST containing 6% skimmed milk powder was used as the blocking solution and stained embryos were mounted in ProLong Gold antifade reagent (Life Technology). For immunohistochemistry, after PFA fixation embryos were embedded in Tissue-Tek O.C.T compound (Sakura) and sectioned (10 μm) using a Leica CM 1950 cryostat (Leica Microsystems). Sections were post-fixed with 4% PFA on ice for 5 min and washed with PBS. Sections were blocked with 3% bovine serum albumin/3% goat serum/0.1% Triton X-100 in PBS. Primary antibodies used were 1:100 rat polyclonal anti-PECAM1 (BD Biosciences, catalogue number 553370, Franklin Lakes), 1:1,000 chicken polyclonal anti-GFP (Abcam, catalogue number ab13970) and 1:5,000 mouse monoclonal α-actinin (Sigma, catalogue number A7811). Secondary antibodies including goat anti-rat, goat anti-chicken or goat anti-mouse (Alexa Fluor-555 or 488; Invitrogen) were used at a dilution of 1:200. Immunofluorescent images were acquired on confocal microscope, Zeiss LSM 700 Upright (Carl Zeiss MicroImaging).

Quantification mouse Cre/loxP lineage tracing. For Cre lineage studies, the *Nkx2-5*^{irescre} strain[14] was crossed either with *Z/EG*[15] or *Rosa*^{YFP} (ref. 16) reporter lines. The number of PECAM1^{+} endothelial cells was counted for each PAA across different embryonic stages (average of 10 sections evaluated per embryo per stage) and the percentages of *Nkx2-5* lineage traced YFP/GFP^{+} cells were determined. We averaged the results across 2 embryos and the error bars represent 1 s.d. from the mean. Total cells counted across two embryos: E9.5 PAA 1, $n = 244$; E10.5 PAA 2, $n = 216$; E10.5 PAA 3, $n = 1{,}357$; E10.5 PAA 3 + aortic sac, $n = 642$; E11.5 PAA 4, $n = 511$; E11.5 PAA 6, $n = 649$.

Mouse PAA patency assessment. Ink injection was performed according to previously described protocols[43,44]. India ink was injected with a pulled capillary tube into the ventricle of E9.5 embryos using a Picospritzer III micro dispenser system (Parker). After injection embryos were placed in relaxation buffer (0.1 mM ethyleneglycol-bis(2-aminoethylether)-*N*,*N*,*N*′,*N*′-tetraacetic acid (EGTA), 30 mM KCl, 0.2 mM verapamil and 10 U ml^{-1} heparin in Hank's balanced salt solution (Invitrogen)) for 1 min. Embryos were then fixed in 95% ethanol/1% acetic acid/1% chloroform overnight followed by graded ethanol dehydration. Embryos were cleared with 1:1 benzyl benzoate and benzyl alcohol and imaged using Leica M125 stereomicroscope (Leica Microsystems).

Statistics and general methods. For all experiments, no statistical method was used to predetermine sample size, the experiments were not randomized, and the investigators were not blinded to allocation during experiments and outcome assessment. Further, all zebrafish animals were included in the analyses unless they exhibited gross morphological defects inconsistent with the experimental treatment. In these instances, dysmorphic animals due to unknown developmental delay (that is, ventralized or dorsalized zebrafish embryos) were excluded equally from control and experimental groups. All mouse animals were included in the analyses.

30. Kikuchi, Y. *et al.* The zebrafish bonnie and clyde gene encodes a Mix family homeodomain protein that regulates the generation of endodermal precursors. *Genes Dev.* **14,** 1279–1289 (2000).
31. Mizoguchi, T., Verkade, H., Heath, J. K., Kuroiwa, A. & Kikuchi, Y. Sdf1/Cxcr4 signaling controls the dorsal migration of endodermal cells during zebrafish gastrulation. *Development* **135,** 2521–2529 (2008).
32. Jin, S. W., Beis, D., Mitchell, T., Chen, J. N. & Stainier, D. Y. Cellular and molecular analyses of vascular tube and lumen formation in zebrafish. *Development* **132,** 5199–5209 (2005).
33. Traver, D. *et al.* Transplantation and *in vivo* imaging of multilineage engraftment in zebrafish bloodless mutants. *Nat. Immunol.* **4,** 1238–1246 (2003).
34. Yaniv, K. *et al.* Live imaging of lymphatic development in the zebrafish. *Nat. Med.* **12,** 711–716 (2006).
35. Staal, J., Abramoff, M. D., Niemeijer, M., Viergever, M. A. & van Ginneken, B. Ridge-based vessel segmentation in color images of the retina. *IEEE Trans. Med. Imag.* **23,** 501–509 (2004).
36. Burns, C. G. *et al.* High-throughput assay for small molecules that modulate zebrafish embryonic heart rate. *Nat. Chem. Biol.* **1,** 263–264 (2005).
37. Long, S. & Rebagliati, M. Sensitive two-color whole-mount *in situ* hybridizations using digoxygenin- and dinitrophenol-labeled RNA probes. *BioTechniques* **32,** 494 (2002) 496, 498 passim.
38. Thisse, C. & Thisse, B. High-resolution *in situ* hybridization to whole-mount zebrafish embryos. *Nat. Protocol.* **3,** 59–69 (2008).
39. Feng, H. *et al.* T-lymphoblastic lymphoma cells express high levels of BCL2, S1P1, and ICAM1, leading to a blockade of tumor cell intravasation. *Cancer Cell* **18,** 353–366 (2010).
40. Marques, S. R., Lee, Y., Poss, K. D. & Yelon, D. Reiterative roles for FGF signaling in the establishment of size and proportion of the zebrafish heart. *Dev. Biol.* **321,** 397–406 (2008).
41. Brand, M. G. & Nüsslein-Volhard, C. *Keeping and Raising Zebrafish* (Oxford Univ. Press, 2002).
42. Prall, O. W. *et al.* An Nkx2-5/Bmp2/Smad1 negative feedback loop controls heart progenitor specification and proliferation. *Cell* **128,** 947–959 (2007).
43. Chapnik, E., Sasson, V., Blelloch, R. & Hornstein, E. Dgcr8 controls neural crest cells survival in cardiovascular development. *Dev. Biol.* **362,** 50–56 (2012).
44. Lorandeau, C. G., Hakkinen, L. A. & Moore, C. S. Cardiovascular development and survival during gestation in the Ts65Dn mouse model for Down syndrome. *Anat. Rec.* **294,** 93–101 (2011).

DOI: 10.1038/ncb2862

nature cell biology

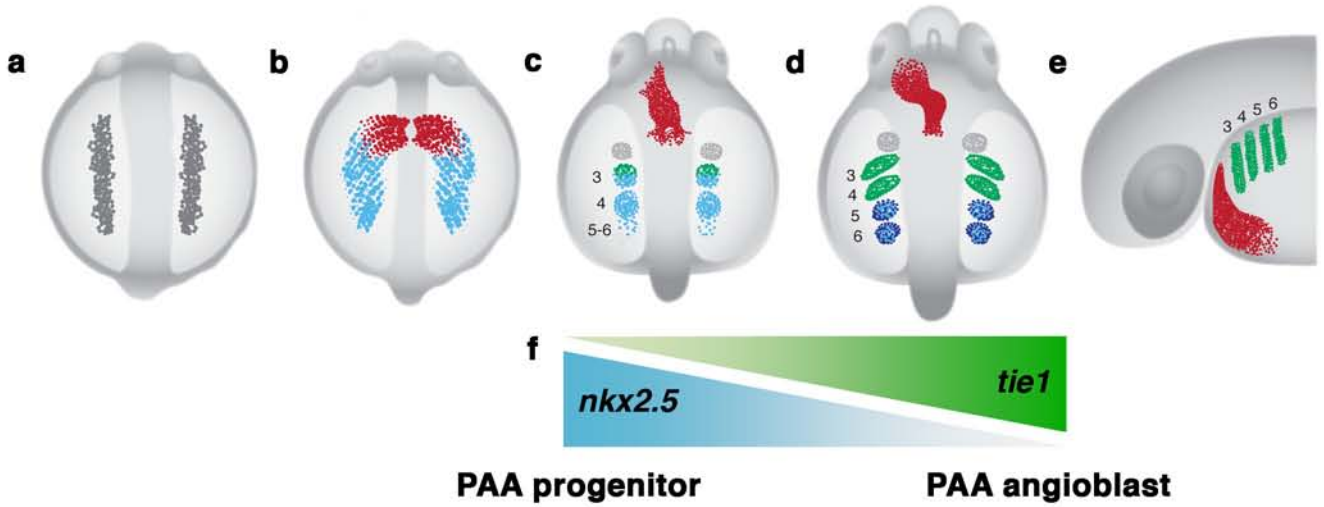

Figure S1 Cartoons depicting *nkx2.5*$^{+}$ heart field origin of PAA endothelium. **a**, At 16 hpf (14ss), the bilateral *nkx2.5*$^{+}$ ALPM (dark gray) contains progenitors for both cardiac and PAA endothelial lineages. **b**, As cardiac progenitors (red) migrate to the midline (18 hpf, 18ss) to form the primitive heart, *nkx2.5*$^{+}$ PAA progenitors (light blue) remain lateral and begin to condense. **c**, As the heart tube elongates (30 hpf), *nkx2.5*$^{+}$ PAA progenitors condense into 3 clusters with diffuse progenitors residing caudally. The anterior-most cluster (light gray) gives rise to non-PAA tissue within the face (data not shown). The 2nd cluster initiates expression of angioblast marker *tie1* (green) and concomitantly downregulates *nkx2.5* prior to forming PAA3. **d**, By 38 hpf, the 3rd cluster similarly adopts a *tie1*$^{+}$ angioblast fate and subsequently forms PAA4. During similar stages, 2 undifferentiated caudal clusters emerge that are comprised of *nkx2.5*$^{+}$ PAA progenitors specified in the heart field (light blue) and PAA progenitors initiating *nkx2.5* expression *de novo* in the pharynx (dark blue). These caudal clusters form PAAs 5 and 6, respectively. **e**, By 60 hpf, PAAs 3-6 (green) are patent vessels expressing markers of terminal endothelial differentiation such as *tie1*, *fli1a*, and *kdrl*, but not the progenitor marker *nkx2.5*. **f**, Schematic diagram depicting the reciprocal relationship between *nkx2.5* and *tie1* expression during the PAA progenitor to angioblast transition. **a**-**d**, dorsal views, anterior up; **e**, lateral view, anterior left; angioblast cluster and corresponding PAA numbers indicated.

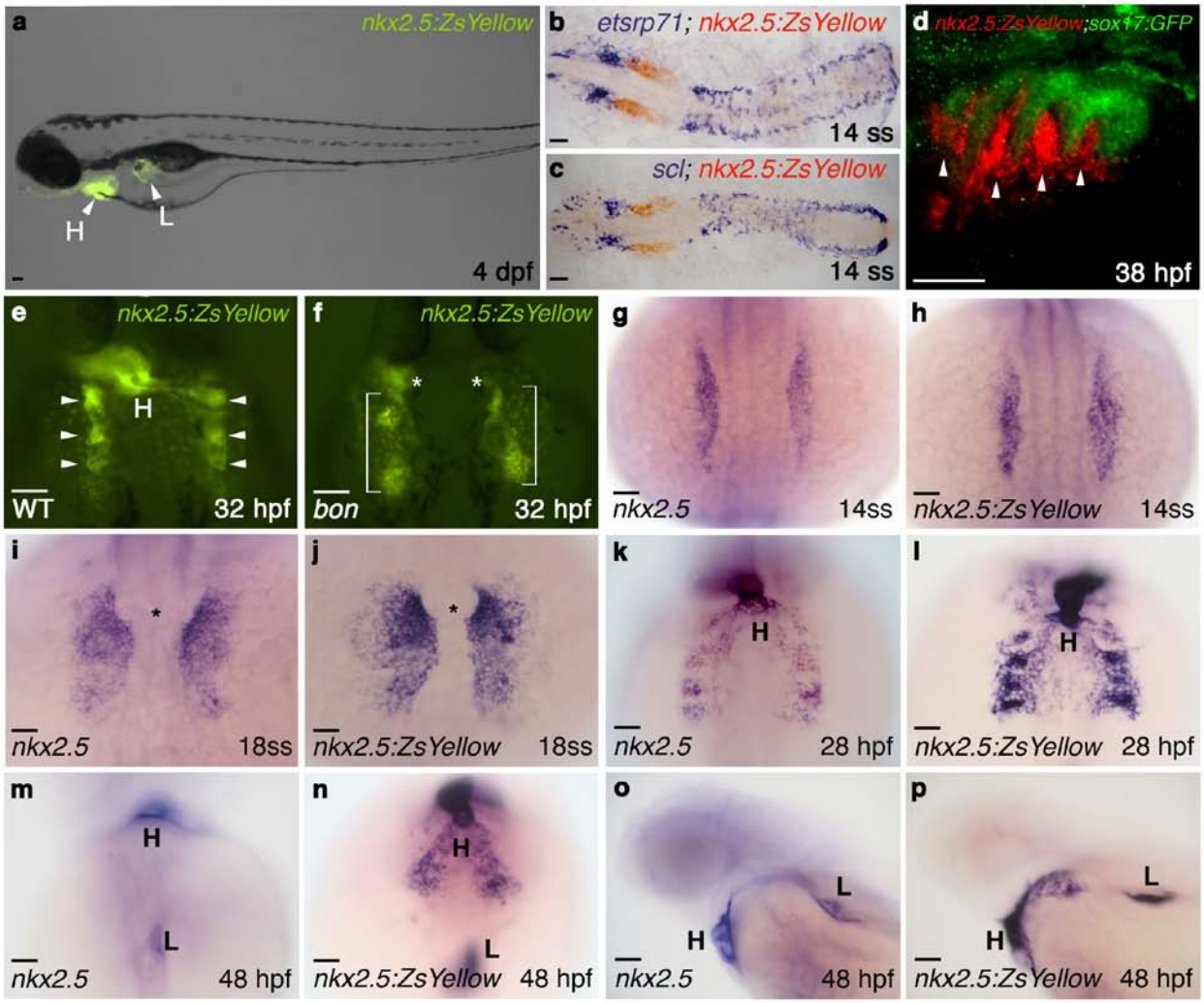

Figure S2 ZsYellow is expressed in the anterior lateral plate and pharyngeal mesoderm of *Tg(nkx2.5:ZsYellow)* in patterns non-overlapping with hemangioblast or endodermal markers**. a**, Gross evaluation of *Tg(nkx2.5:ZsYellow)* embryos at 4 dpf revealed robust ZsYellow fluorescence in the heart (H) and liver (L). **b**,**c**, *ZsYellow* transcripts (red) were detected in the anterior lateral plate mesoderm (ALPM), abutting hemangioblast markers *etsrp71* (**b**) and *scl* (**c**). **d**, *Tg(nkx2.5:ZsYellow)*; *Tg(sox17:GFP)* embryo immunostained with anti-ZsYellow and anti-GFP antibodies to highlight *nkx2.5*$^{+}$ pharyngeal cells (red) and *sox17*$^{+}$ pharyngeal endoderm (green), respectively. Red-only *nkx2.5*$^{+}$ clusters (arrowheads) were detected in between green-only *sox17*$^{+}$ endodermal pouches. **e**,**f**, ZsYellow^{+} populations were examined in endoderm-less *bonnie and clyde* (*bon*); *Tg(nkx2.5:ZsYellow)* embryos and their phenotypically wild-type (WT) siblings. A midline heart and bilateral pharyngeal clusters (arrowheads) were detected in WT siblings. *bon* mutants exhibited cardia bifida (asterisks) and significant populations of bilateral pharyngeal ZsYellow^{+} cells (brackets), demonstrating their non-endodermal nature. The un-clustered appearance of ZsYellow^{+} PAA progenitor cells in *bon* embryos likely reflects their lack of pharyngeal segmentation. WT, *n*=78; *bon*, *n*=25. **g**-**p**, Spatiotemporal comparison of endogenous *nkx2.5* and *ZsYellow* transcripts in wild-type and *Tg(nkx2.5:ZsYellow)* embryos. Transcripts for *nkx2.5* and *ZsYellow* were indistinguishable at 14ss (**g**,**h**), 18ss (**i**,**j**) and 28 hpf (**k**,**l**). While *nkx2.5* transcripts disappeared specifically from pharyngeal mesoderm by 48 hpf (**m**,**o**), ZsYellow transcripts persisted in this region reflecting higher ZsYellow transcript stability (**n**,**p**). **a**,**d**,**o**,**p** lateral views, anterior left; **b**,**c** flat-mount dorsal views, anterior left; **e**-**n** dorsal views, anterior up; **a**-**d**, **g**-**p** *n*>20 embryos per group. Scale bar = 50 μm. Abbr: H, heart; L, liver.

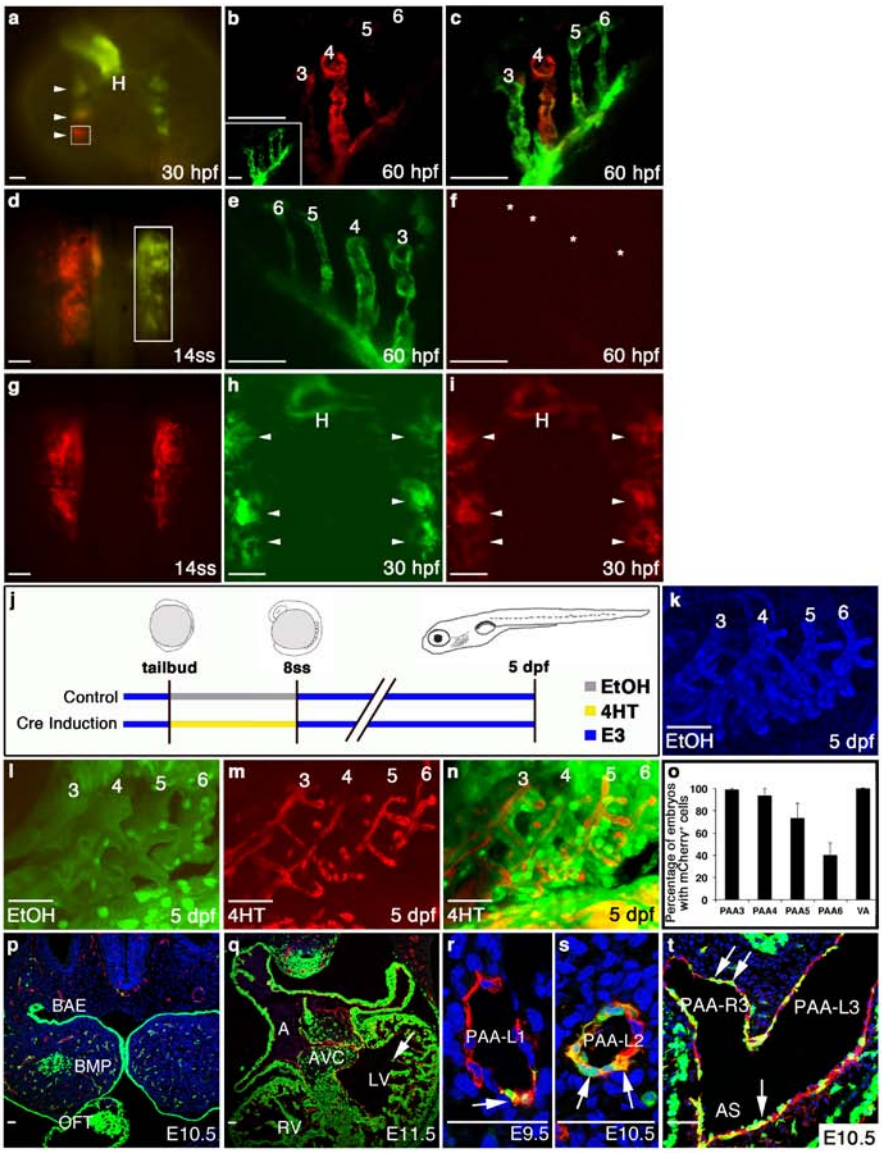

Figure S3 Fate mapping and genetic lineage tracing of *nkx2.5*$^{+}$ cells. **a**-**i**, *nkx2.5*$^{+}$ pharyngeal clusters are derived from the heart field and give rise to PAA endothelium. **a**-**c**, Kaede photoconversion of cluster 3 (white box) at 30 hpf. Embryos were imaged in the green and red channels immediately after photoconversion (merged image is shown in **a**) and again at 60 hpf [green (inset, **b**), red (**b**) and merged images (**c**) are shown; *n*=2]. Cluster 3 gave rise predominately to endothelium in PAA4 with a minimal contribution to PAA5 (**b**,**c**). **d**-**f**, When the left ALPM was photoconverted as shown in Figure 2k, the right ALPM (**d**) was left unconverted (white box) as a contralateral control. Embryos were imaged in the green and red channels immediately after photoconversion (merged image is shown in **d**) and subsequently at 60 hpf [green (**e**) and red (**f**) images are shown; (*n*=2)]. No red reporter fluorescence was detected in the right side PAAs (asterisks in **f**). **g**-**i**, *Tg(nkx2.5:Kaede)* embryos were pan-photoconverted at 14ss and immediately imaged in the green and red channels (merged image is shown in **g**) and subsequently at 30 hpf [green (**h**) and red (**i**) images are shown; *n*=3]. Red reporter fluorescence was detected in the heart tube (H) and three bilateral pairs of pharyngeal clusters (arrowheads, *n*=3). **j**-**t**, Genetic lineage tracing of *nkx2.5*$^{+}$ progenitors. **j**, Cartoon depicting vehicle control (EtOH; gray bar) or 4HT (yellow bar) treatment of *Tg(nkx2.5:ERCre^{T2})*; *Tg(kdrl:CSY)* or *Tg(nkx2.5:ERCre^{T2})*; *Tg(ubi:Switch)* zebrafish embryos between tailbud and 8ss (10-13 hpf). Following extensive washing with fresh E3, embryos were incubated until 5 dpf and evaluated for reporter expression. **k**, Merged blue and yellow confocal z-stacks showing PAAs 3-6 in an EtOH-treated *Tg(nkx2.5:ERCre^{T2})*; *Tg(kdrl:BSY)* embryo. Yellow reporter fluorescence was not detected (*n*=80), across three experimental replicates. **l**, Merged green and red confocal z-stacks showing PAAs 3-6 in an EtOH-treated *Tg(nkx2.5:ERCre^{T2})*; *Tg(ubi:Switch)* control embryo. Red reporter fluorescence was not detected (*n*=80). **m**,**n**, Red (**m**) and merged (**n**, red and green) confocal z-stack images showing PAAs 3-6 in a 4HT-treated *Tg(nkx2.5:ERCre^{T2})*; *Tg(ubi:Switch)* embryo. Robust red reporter fluorescence was detected in PAAs 3-6 and the quantification is shown in **o**, *n*=75 total across three experimental replicates. Error bars equal one standard deviation. **p**-**t**, Embryos derived from *Nkx2-5^{IRESCre}* driver and *ROSA^{YFP}* (**q**,**r**,**s**,**t**) or *Z/EG* (**p**) reporter line crosses co-stained with PECAM1 (red) and DAPI (blue). Embryos immunostained with anti-GFP (green) and anti-PECAM1 (red) antibodies showed contributions of Nkx2-5-lineage traced cells to the myocardium, endocardium, BAE and BMP (**p**,**q**, *n*=2). **r**-**t**, Arrows indicate YFP^{+}PECAM^{+} lineage traced endothelial cells. **t**, YFP^{+} lineage traced endothelial cells at the junction between the Aortic Sac (AS) and the left and right sides of PAA3. Cells counted across two embryos: E9.5 (PAA 1, *n*=244), E10.5 (PAA 2, *n*=216, PAA 3, *n*=1357, PAA3 + aortic sac, *n*=642). **a**,**d**,**g**-**i** dorsal views, anterior up; **b**,**c**,**e**,**f**,**k**-**n** lateral views, anterior left; **p**-**t**, coronal sections. Scale bar = 50μm. Abbr: ss, somite stage; EtOH, ethanol; 4HT, 4-hydroxytamoxifen; dpf, days post-fertilization; A, atrium; AVC, atrio-ventricular canal; RV, right ventricle; LV, left ventricle; BAE branchial arch epithelium; BMP, branchial myogenic plate; OFT, outflow tract; AS, aortic sac; PAA number and left (L) and right (R) designations indicated.

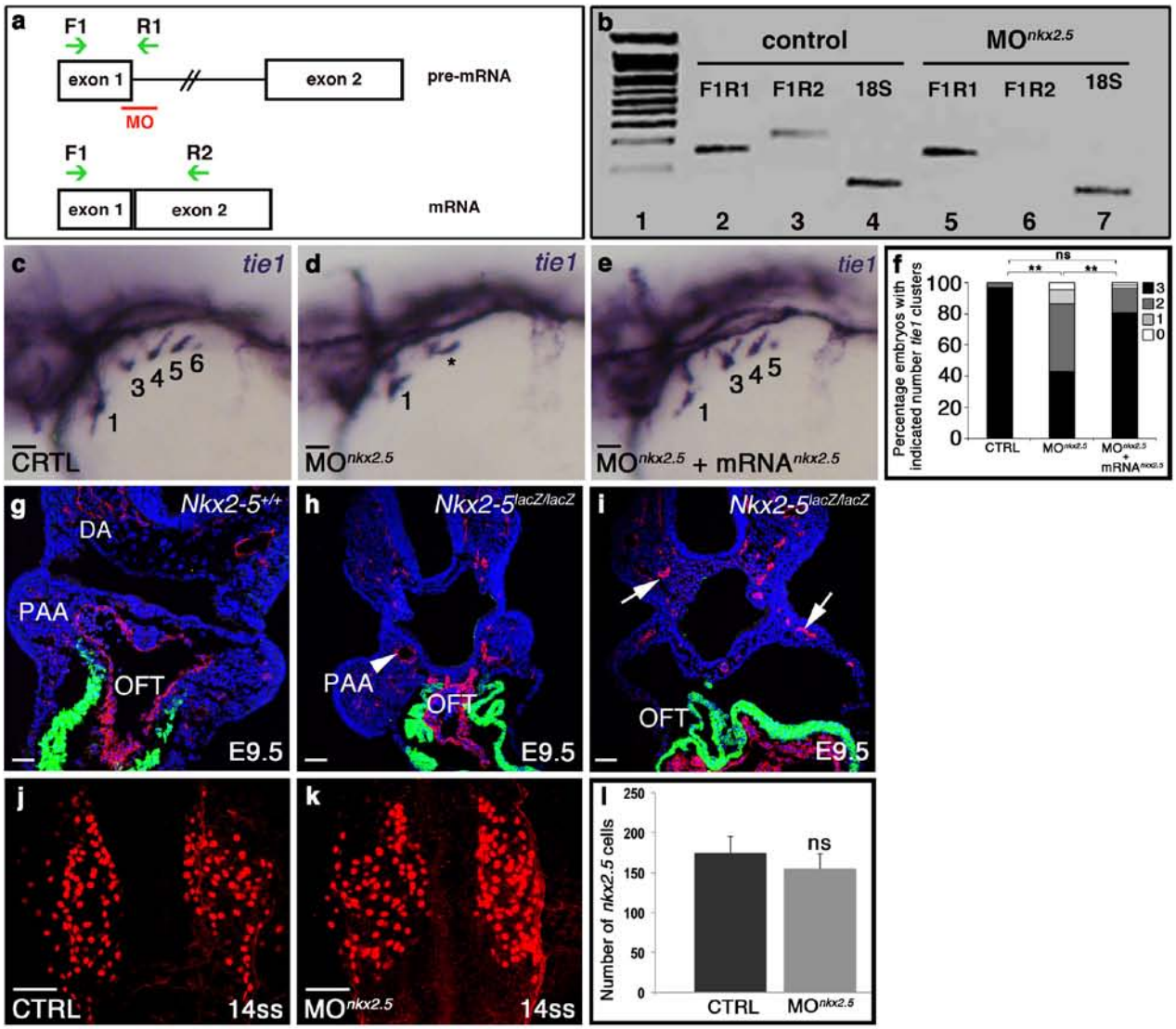

Figure S4 *nkx2.5* mutant and knock-down phenotypes in mice and zebrafish, respectively. **a**-**f**, Validation of the *nkx2.5*antisense morpholino. **a**, Schematic diagram of the *nkx2.5* pre-mRNA and mature mRNA transcripts. The morpholino target site (MO, red bar) and the primer pairs used for RT-PCR (green arrows) are shown. **b**, Agarose gel of RT-PCR amplification products from control and *nkx2.5* morphant ($MO^{nkx2.5}$) 28 hpf embryos. While both control and *nkx2.*5 morphant embryos contained pre-mRNA transcripts (primer pair F1R1, 189 bp amplicon, lanes 2 and 5), *nkx2.*5 morphant embryos lacked spliced mRNA transcripts (primer pair F1R2, 230 bp amplicon, lanes 3 and 6). Lane 1 contains a 100 bp molecular weight ladder, and lanes 4 and 7 contain 18S rRNA loading controls. **c**-**e**, *in situ* hybridization analysis of *tie1* transcripts revealed fewer PAA angioblast clusters in morphant (**d**, *n*=65) when compared to control embryos (CTRL **c**, *n*=33). The asterisk in (**d**) labels a single PAA angioblast. This phenotype was rescued by co-injection of 50 pg full-length zebrafish *nkx2.5* mRNA (**e**, $mRNA^{nkx2.5}$ *n*=57). **f**, Phenotypic quantification and rescue; two-tailed *t* test, $^{**}P$=0.001, no significant (ns, *P*=0.0755) difference was observed between CTRL and *nkx2.5* morphants rescued with *nkx2.5* mRNA. **g**-**i**, Section immunofluorescence analysis of $Nkx2\text{-}5^{+/+}$ (**g**) and $Nkx2\text{-}5^{lacZ/lacZ}$ (**h**,**i**) embryos at E9.5 highlighting $PECAM^{+}$ endothelium (red), alpha-$actinin^{+}$ outflow tract (OFT) myocardium (green), and $DAPI^{+}$ nuclei (blue) (*n*=5 per group). $Nkx2\text{-}5^{lacZ/lacZ}$ embryos contain $PECAM1^{+}$ endothelial cells in rudimentary PAA lumens (arrowhead, **h**) or scattered in regions where the dorsal aorta (DA) and 3rd PAA would otherwise form (arrows, **i**). **d**-**e**, Confocal z-stack images of flat-mounted control (**j**) and *nkx2.5* morphant ($MO^{nkx2.5}$; **k**) *Tg(nkx2.5:nZsYellow)* embryos at 14ss immunostained for ZsYellow protein (red). **l**, Graph depicting quantification of $nkx2.5^{+}$ nuclei in the ALPM of control (*n*=5) and $MO^{nkx2.5}$ (*n*=6) embryos. No significant (ns) difference was observed across two independent experiments. Error bars equal one standard deviation, two-tailed *t* test *P*=0.1219. **c**-**e** lateral views, anterior up; **g**-**i** coronal sections; **j**,**k** flat-mounted dorsal views, anterior up. Scale bar = 50μm. Abbr: OFT, outflow tract; DA, dorsal aorta.

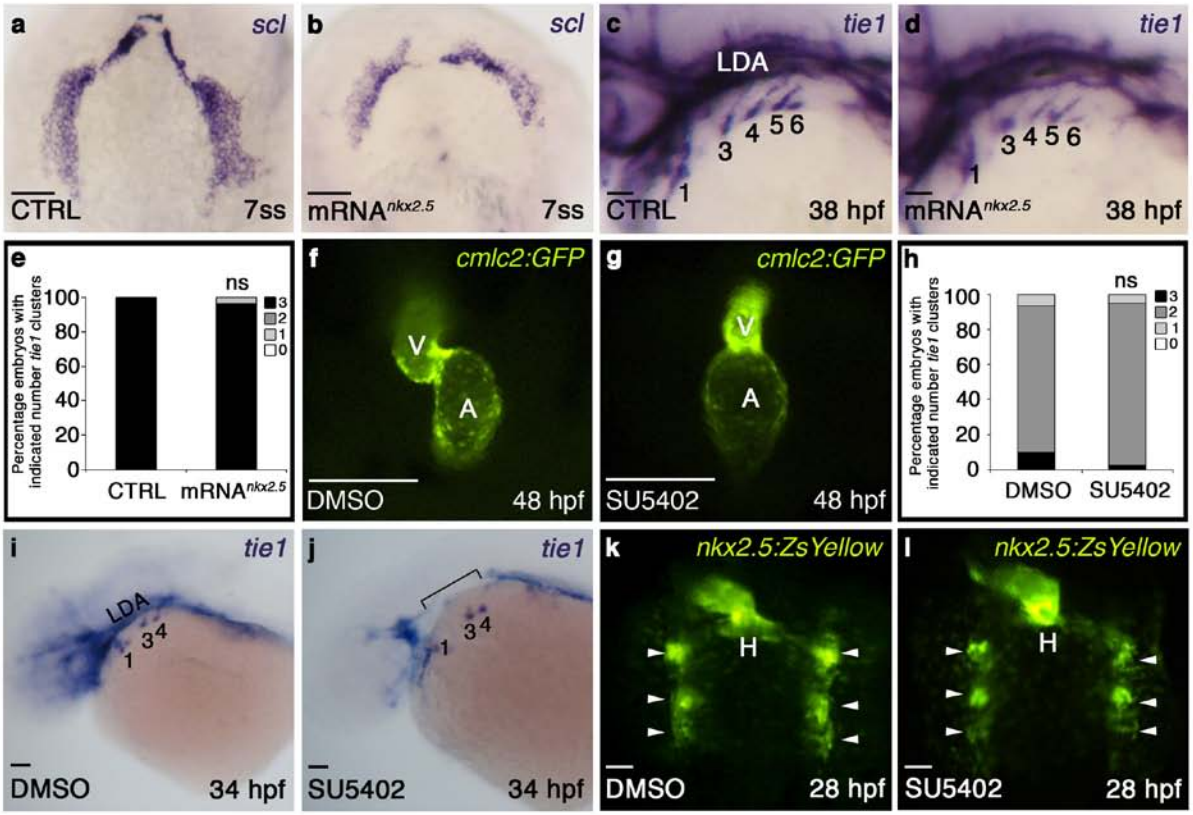

Figure S5 Neither overexpression of *nkx2.5* nor inhibition of FGF signaling suppresses PAA endothelial cell differentiation. **a**-**e**, Embryos were injected with 100 pg full-length *nkx2.5* mRNA (mRNA$^{nkx2.5}$) and evaluated by *in situ* hybridization for *scl* expression in the ALPM at 7ss (**a**,**b**) or *tie1* expression in pharyngeal clusters at 38 hpf (**c**,**d**). Expression of *scl* was severely reduced in the ALPM of *nkx2.5* mRNA injected embryos (**b**) (n>20 per group). No significant (ns) difference (**e**) in the number of *tie1*-expressing PAA clusters was observed between control (**c**, n=16) and *nkx2.5* injected embryos (**d**, n=26; two-tailed t test, P=0.4481) across two experimental replicates. **f**,**g** *Tg(cmlc2:EGFP)* embryos were treated with DMSO or the FGF inhibitor SU5402 (10 μM) starting at 5ss and imaged at 48 hpf. Treated embryos exhibited a small ventricle, a phenotype known to arise from inhibition of FGF signaling. **h**-**l**, *Tg(nkx2.5:ZsYellow)* embryos were treated with DMSO and SU5402 (10 μM) beginning at the 5ss and imaged at 28 hpf (**k**,**l**) or fixed at 34 hpf for *in situ* hybridization (**i**,**j**). *in situ* hybridization for *tie1* revealed equal numbers of PAA angioblast clusters (**h**) between control (**i**) and treated (**j**) embryos, (DMSO, n=30; SU5402, n=38; two-tailed t test, P=0.7254 across two experimental replicates). Interestingly, FGF-deficient embryos exhibited disrupted body vasculature as demonstrated by the absence of vessels in the eye and the LDA (bracket). ZsYellow^{+} clusters in the pharynx (arrowheads) were indistinguishable between control (**k**) and treated (**l**) animals, demonstrating effective segregation of the PAA and cardiac progenitors (n>20 per group). **a**,**b**,**k**,**l** dorsal views, anterior up; **c**,**d**,**i**,**j** lateral views, anterior left; **f**,**g** ventral views. Scale bar = 50μm. Abbr: H, heart; LDA, lateral dorsal aorta; V, ventricle; A, atrium.